



Review

Kinetic and mechanistic aspects of metallocene polymerisation catalysts

Manfred Bochmann *

Wolfson Materials and Catalysis Centre, School of Chemical Sciences and Pharmacy, University of East Anglia, University Plain, Norwich NR4 7TJ, UK

Received 4 May 2004; accepted 1 July 2004
Available online 12 August 2004

Dedicated to Prof. Dr. G. Fink on the occasion of his 65th birthday

Abstract

The nature of the counteranion is an essential component of metallocene polymerisation catalysts. Detailed mechanistic investigations show how the anion is able to determine the activity and, in many cases, also the stereoselectivity of the catalyst. This review summarises recent advances in mechanistic understanding of well defined metallocene catalysts based on ion pairs $[L_2ZrR^+ \cdots X^-]$ and describes recent insights in ion mobility and kinetics of alkene polymerisation processes. The interplay of ligand structure and nature of the counteranions demonstrates a fascinating versatility and subtlety that continually challenge our ability to rationalise and predict catalyst performance.

© 2004 Elsevier B.V. All rights reserved.

Keywords: Catalysis; Metallocenes; Polymerisation; Anion effects; Kinetics; Stereoselectivity

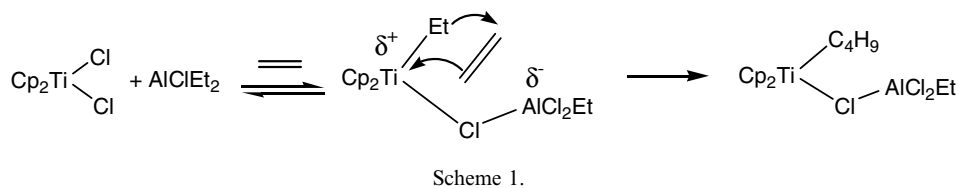
1. Introduction

At the 40th anniversary of the *Journal of Organometallic Chemistry* it is appropriate to recall two other current anniversaries that have contributed so much to the development of organometallic chemistry. The year 1953 saw the birth of two important newcomers to this world whose fate, as it turned out, were to become intricately linked: on 15 January 1953 Wilkinson et al. [1] submitted their communication on the synthesis of Cp_2TiBr_2 and Cp_2ZrBr_2 , and on 26 October 1953 the low-pressure polymerisation of ethylene with “Ziegler catalysts” ($TiCl_4/AlEt_3$) was discovered [2], to be followed a very short time later, on 11 March 1954, by Natta’s discovery of polypropylene [3]. Within a year the infants were introduced to each other: the potential of

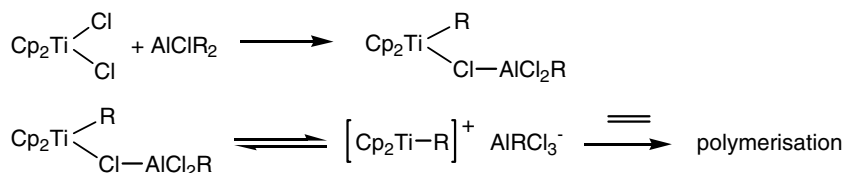
titanocene complexes as alkene polymerisation catalysts was explored as early as 1955, not least because these homogeneous catalysts were more amenable to mechanistic investigation and were likely to throw some light on the processes operative in Ziegler catalysts [4,5]. Some key mechanistic features were soon realised: (i) the need for Lewis acidic main group alkyls as activators, which can form complexes with the inactive catalyst precursor and are capable of transferring an alkyl ligand to the transition metal [6]; (ii) the importance of the appropriate activator to maximise catalytic activity, (iii) oxidation state IV for the active species and reduction as a deactivating side reaction [6,7]; (iv) polymer chain growth by monomer insertion into a Ti–alkyl bond [7]; (v) the equilibrium nature of the reactions leading to the active species; (vi) reversible alkyl ligand transfer to aluminium, and (vii) an intermittent chain growth behaviour, with an equilibrium between active and dormant states [8]. Initiation, propagation and

* Tel./fax: +44 1603 592044.

E-mail address: m.bochmann@uea.ac.uk.



Scheme 1.



Scheme 2.

termination rates and the time dependence of the number-average molecular weight were measured using ($^{14}\text{CH}_3$) $_2\text{AlCl}$ isotopic labelling [9].

While Breslow's mechanistic suggestions (Scheme 1) involved a zwitterionic species and adhered to a tetrahedral geometry for the titanium centre [6,7], alternative suggestions were made, such as octahedral intermediates suggested by Henrice-Olivé and Olivé [10]. An early proposal by Zefirova and Shilov [11] that the active species was likely to be cationic (Scheme 2) received little attention until the advent of well-defined polymerisation catalysts based on metallocenium salts in the mid-1980s [12–15]. The discovery of methylaluminoxane (MAO) as a more effective activator by Sinn and Kaminsky [16] and the development of *ansa*-metallocenes by Brintzinger [17] provided the basis for modern high-activity metallocene catalysts.

This brief review attempts to summarise some recent advances in the mechanistic understanding of metallocene polymerisation catalysts. For a fuller account of the chemistry of metallocene catalysts the reader is referred to a series of excellent recent reviews [18–26].

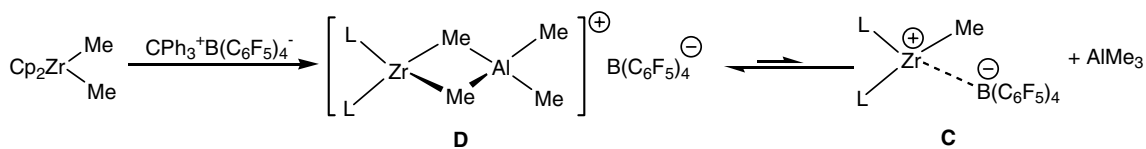
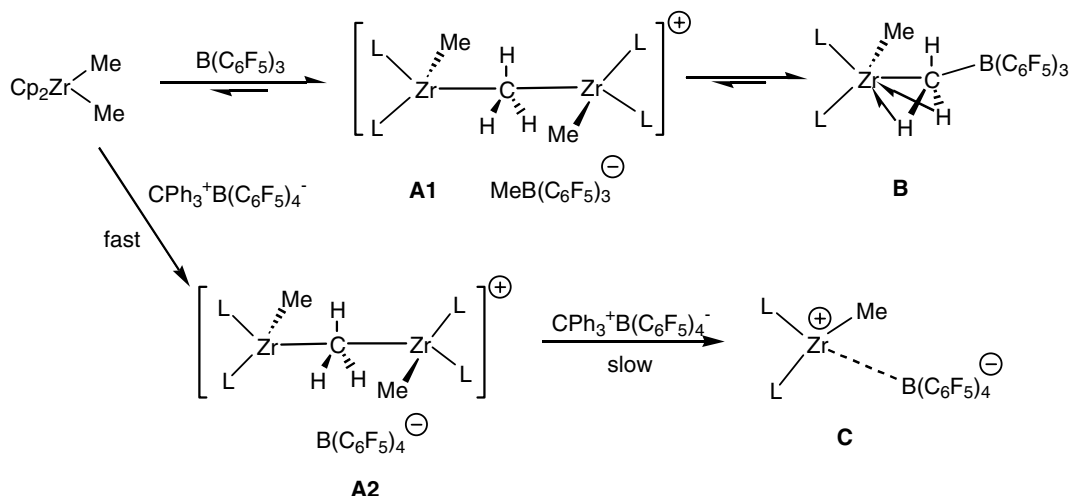
2. Dramatis personae: structural principles of cationic metallocene species

It is now well recognised that the active species is a cationic complex, or more precisely an ion pair, $[\text{L}_2\text{M}-\text{R}^+\cdots\text{X}^-]$ [15,27]. Such species can be generated from group 4 metallocene dichlorides and MAO, or from metallocene dialkyls and cation generating agent such as $\text{B}(\text{C}_6\text{F}_5)_3$, $\text{HNMe}_2\text{Ph}^+\text{B}(\text{C}_6\text{F}_5)_4^-$ or $\text{CPh}_3^+\text{B}(\text{C}_6\text{F}_5)_4^-$ [15,19,21,28]. Boron- C_6F_5 compounds are characterised by chemical robustness and resistance to hydrolysis [29], and their use in metallocene polymerisation catalysis [30,31] led to highly active catalyst systems that were amenable to mechanistic studies. Since this aspect has been dealt with in earlier reviews, only a brief summary

is given here. While methide-abstraction from L_2ZrMe_2 with $\text{B}(\text{C}_6\text{F}_5)_3$ gives zwitterionic products of molecular structure, $\text{L}_2\text{ZrMe}(\mu\text{-Me})\text{B}(\text{C}_6\text{F}_5)_3$ (**B**, Scheme 3), the reaction of L_2MMe_2 with $[\text{CPh}_3][\text{B}(\text{C}_6\text{F}_5)_4]$ proceeds in stages to give initially homobinuclear cations $[(\text{L}_2\text{MMe})_2(\mu\text{-Me})]^+$ (**A2**) which react with further CPh_3^+ in a subsequent but much slower reaction to give ion pairs of type **C**. The chemistry of the highly electron-deficient 14-electron species $[\text{L}_2\text{MMe}]^+$ is dominated by equilibria [32], including the formation of **B** via intermediate **A1** [33]. The formation of **A2** can be regarded as instantaneous even at low temperatures [32], while the formation of **C** with excess is comparatively slow, depending on the ligand system. With $\text{L}_2 = \text{rac-Me}_2\text{-Si}(\text{Ind})_2$ (SBI) in benzene- d_6 at 298 K, the conversion of **A2** into **C** under pseudo-first order conditions proceeded with a rate $k = 3 \times 10^{-4} \text{ s}^{-1}$ [34].

If other sufficiently basic and sterically unhindered metal alkyls are present, such as Al_2Me_6 , heterobinuclear adducts **D** result (Scheme 4) [32]. The identification of these species is of obvious relevance to the catalyst speciation in systems activated by MAO which typically contains substantial amounts (ca. 30%) of Al_2Me_6 . The cation **D** and species related to **C** have subsequently been identified in MAO-activated metallocenes, e.g., using ^{13}C -labelled MAO [35,36].

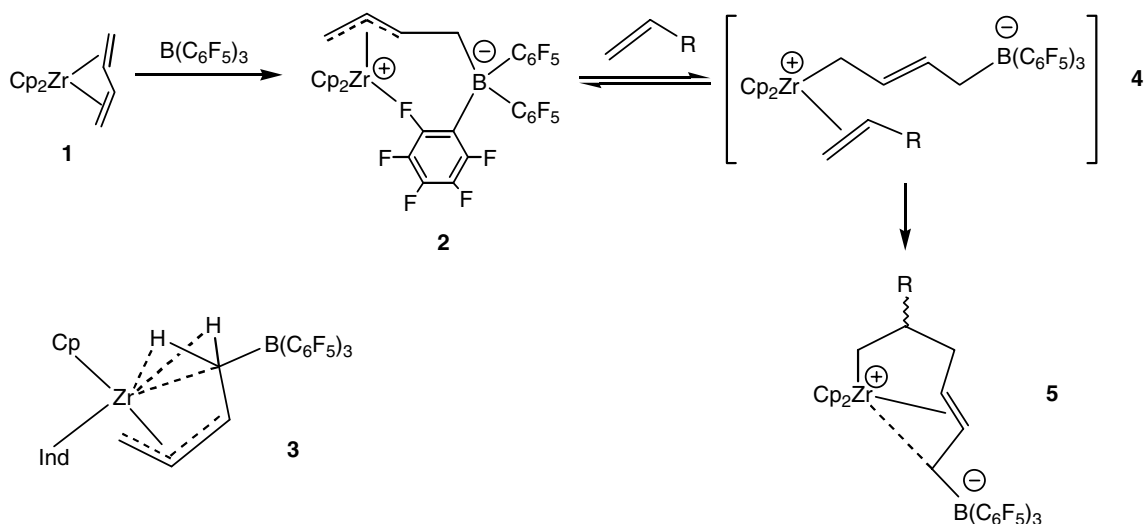
Both **A** and **D** are catalytically active, even though a neutral metal complex (i.e., L_2ZrMe_2 and AlMe_3 , respectively) occupies the coordination site necessary for alkene binding. One has to assume, therefore, that both these species are part of a dissociation equilibrium with the “naked” ion pair **C**. If so, additional AlMe_3 should have a negative effect on catalyst activity; this was indeed shown to be the case [32,37]. Dissociation becomes more favourable with increasing bulkiness of AlR_3 ; for example, the AlEt_3 adduct of $[\text{Cp}_2\text{HfEt}]^+$ dissociates more readily and is consequently catalytically more active than the AlMe_3 adduct. Bulkier aluminium alkyls do not appear to form such adducts; e.g., there is no



evidence for Zr–Al complexes of AlBu_3^i (TIBA) which is an excellent co-activator and scavenger in $\text{CPh}_3^+ \text{B}(\text{C}_6\text{F}_5)_4^-$ activated systems. However, while it is conceivable that the inability of TIBA to form stable adducts of type **D** contributes to the high catalytic activity of such systems, the chemistry of TIBA/metallocene mixtures is complex, and other reaction pathways may operate here.

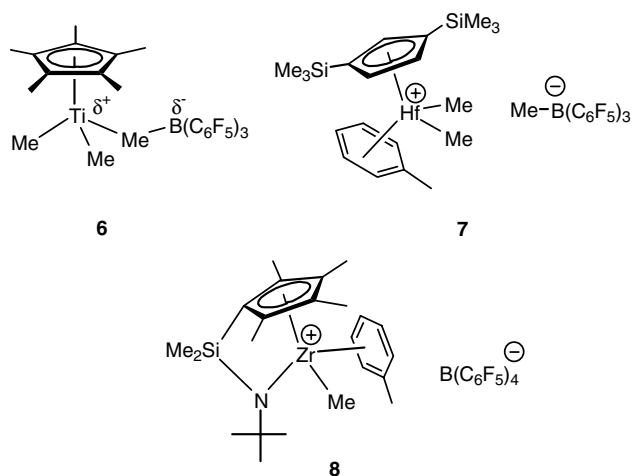
Apart from the formation of **B**, several other modes of activating complexes with $\text{B}(\text{C}_6\text{F}_5)_3$ have been demonstrated, notably the attack at a terminal CH_2 moi-

ety in the *s-trans* diene complex **1** to give zwitterionic zirconocene allyl complexes **2**. If $\text{B}(\text{C}_6\text{F}_5)_3$ adds to the *s-cis* diene isomer, agostically stabilised complexes without $\text{Zr} \cdots \text{F}$ coordination result, for example **3** (Scheme 5). Complexes of type **2** have proved useful for studying the energetics of monomer insertion since at low temperature they react with 1-alkenes to give a mono-insertion product **5**, probably via a σ -allyl alkene complex **4**. Alkene coordination takes place in a pre-equilibrium step, followed by rate-limiting alkene insertion, which tends



to be about 2 kcal/mol higher than the dissociation activation energy [38].

The structural and reaction chemistry outlined for metallocenes cannot necessarily be transferred to half-sandwich complexes. In these more open systems solvent coordination becomes more important and may even outweigh anion coordination. For example, while Cp^*TiMe_3 reacts with $\text{B}(\text{C}_6\text{F}_5)_3$ in toluene to give **6**, the zirconium and hafnium analogues form ionic toluene complexes **7** [39,40]. The crystal structures of the $\text{C}_5\text{H}_3(\text{SiMe}_2)_2$ and Cp^* compounds confirm η^6 -toluene coordination and the absence of close contacts with the anion. Toluene coordination is thought to be responsible for the inferior polymerisation activity of **7** compared to **6** [41,42]. A similar arene complex is formed in the case of the “constrained-geometry” zirconium complex **8** after activation of CGCZrMe_2 with $[\text{CPh}_3][\text{B}(\text{C}_6\text{F}_5)_4]$ [43].

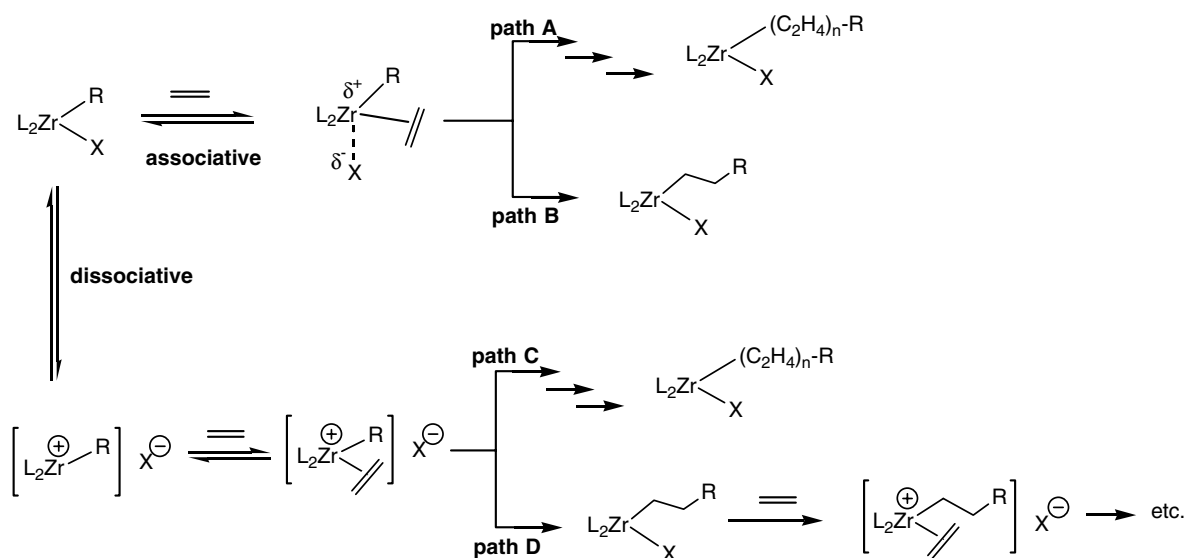


3. Ion pair dynamics in metallocene catalysts

The initiation of the polymerisation process requires the displacement of the anion and coordination of the alkene. The nature of this anion mobility has therefore become the focus of a number of detailed investigations. Questions to be answered are: How fast is anion mobility? Is it faster or slower than monomer binding and chain formation? Is this process associative or dissociative (Scheme 6)? What are the stereochemical consequences of anion mobility on the polymer structure?

Several scenarios are possible:

- (i) The anion dissociates, generating a vacant coordination site on the metal centre which then picks up a monomer molecule for subsequent enchainment. This dissociative model has been favoured in the past [15,19–21,25–29] since it allows a convenient explanation of the observed polymer stereochemistry by considering only the ligands of the cationic metallocene complex. However, anion dissociation must be questioned since in non-polar solvents charge separation is energetically expensive.
- (ii) Even if anion dissociation can be shown to be prevalent, there will be a tendency for anion re-association. This process may be fast or slow relative to the rate of propagation: if it is slow, monomer enchainment may proceed rapidly without anion participation (Scheme 6, path C); if it is fast, the anion will interrupt chain growth after each insertion step, possibly forming long-lived resting states (path D). Which mechanism applies?



Scheme 6.

(iii) In view of the cost in electrostatic energy, it is conceivable that anion dissociation does not take place in the type of hydrocarbon solvents typically used in polymerisation catalysis. Monomer binding will then follow an associative substitution pathway. In that case the anion has to be regarded as an additional, and very bulky, ligand; this will have consequences for the stereoselectivity of 1-alkene polymerisations.

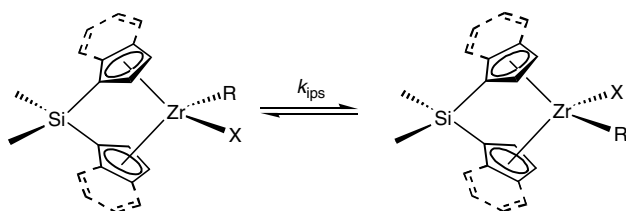
Evidence for anion mobility comes from the exchange process shown in Scheme 7, observed by NMR techniques [25,28,44,45]. In principle, in such a system there are productive and non-productive exchange processes, i.e., those where R and X change positions and those where the starting complex is re-formed; only the former pathway, ion pair symmetrisation, is of course spectroscopically observable and described by the ion-pair symmetrisation rate constant k_{ips} . The process can be conveniently monitored using suitable Cp substituents or, if present, the bridge-SiMe₂ resonances as reporter signals [46].

Brintzinger and co-workers [45] have recently reinvestigated these processes, using complexes of the more strongly coordinating MeB(C₆F₅)₃[−] anion (Scheme 3 type B) and the analogous, more ionic B(C₆F₅)₄[−] compounds (Scheme 3, type C). For a series of *ansa*-metallocenes Me₂Si(L)₂ZrMe(μ-Me)B(C₆F₅)₃ in C₆D₆ at 300 K, apparent first-order rate constants k_{app} are of the order of 1–3 s^{−1}, although those for L = 2-Me-4-Bu^tC₅H₂ are an order of magnitude higher. Generally rates increased with increasing zirconium concentration (2–20 mmol/L), as well as on addition of Li⁺MeB(C₆F₅)₃[−]. The exchange rates for the analogous B(C₆F₅)₄[−] ion pairs were about two orders of magnitude higher (recalculations from the given activation parameters lead to $k_{\text{app}} \approx 200\text{--}300\text{ s}^{-1}$ at 300 K). Differences in rates between the MeB(C₆F₅)₃[−] and B(C₆F₅)₄[−] systems were mainly due to entropy. In effect, the polarised but essentially molecular complexes L₂ZrMe(μ-Me)B(C₆F₅)₃ require much higher concentrations before they form

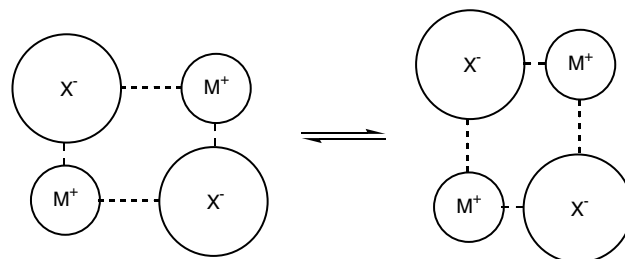
aggregates and display ionic-like exchange rates than B(C₆F₅)₄[−] salts. This difference in polarity and exchange behaviour is of course reflected in the well-known differences in solubility of the two systems and in their propensity for phase separation, i.e., MeB(C₆F₅)₃[−] compounds give homogeneous solutions in toluene even at high concentrations, whereas B(C₆F₅)₄[−] compounds tend to lead to droplet formation and oily precipitates.

Brintzinger suggested an anion exchange process via ion quadruples or higher aggregates, as in Scheme 8. Such a mechanism is attractive in the sense that any energy costs incurred by elongation of the M⁺⋯X[−] distance of one ion pair is compensated by an energy gain as X[−] approaches the neighbouring metal centre of another ion pair, i.e., ion exchange becomes a concerted process. The suggestion of ion quadruple formation was further supported by diffusion coefficient measurements which suggested the existence in benzene solution of ion aggregates larger than simple ion pairs [47].

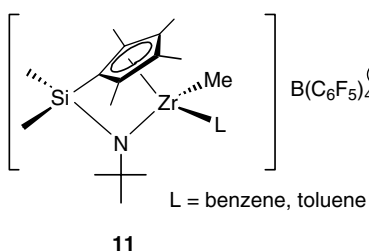
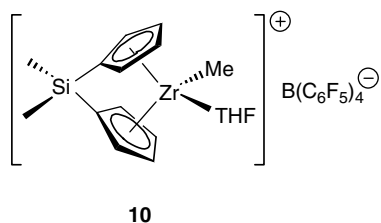
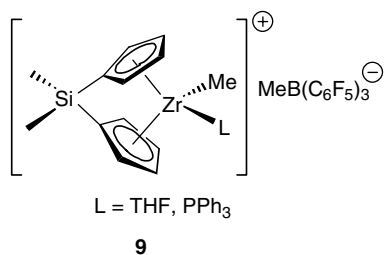
These suggestions have not been without criticism, the objection being that these studies were carried out at significantly higher concentrations than are typically employed under catalytic conditions. Cryoscopic and NMR studies did indeed confirm that methylborate complexes L₂ZrMe(μ-Me)B(C₆F₅)₃, as well as Cp₂ThMe⁺B(C₆F₅)₄[−], exist in solution as simple tight ion pairs [48]. Zirconocenium B(C₆F₅)₄[−] salts (Scheme 3, type C) are less accessible and were not measured. On the other hand, NMR studies showed that outer-sphere ion pairs, where direct contact between cation and anion is prevented by firmly bonded donor ligands or solvents, as in 9–11, have a tendency to form ion quadruples or even hexuples at higher concentrations. Clearly the ionic character of the ion pair, rather than the nature of the anion, is important for aggregation [49]. Since similar structures will be formed when an alkene is coordinated (L = H₂C=CHR), the solution structures of these ion pairs are informative, although the overall trends suggest that at catalytic concentrations (e.g., [Zr] = 10^{−5}–10^{−6} M) ion pairs rather than ion aggregates may prevail.



Scheme 7.

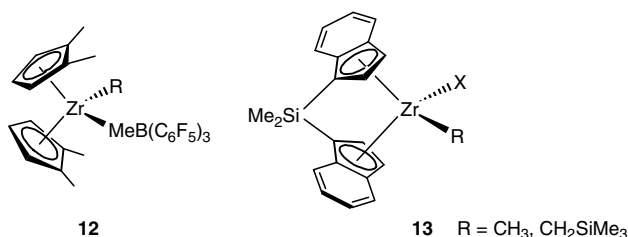


Scheme 8.

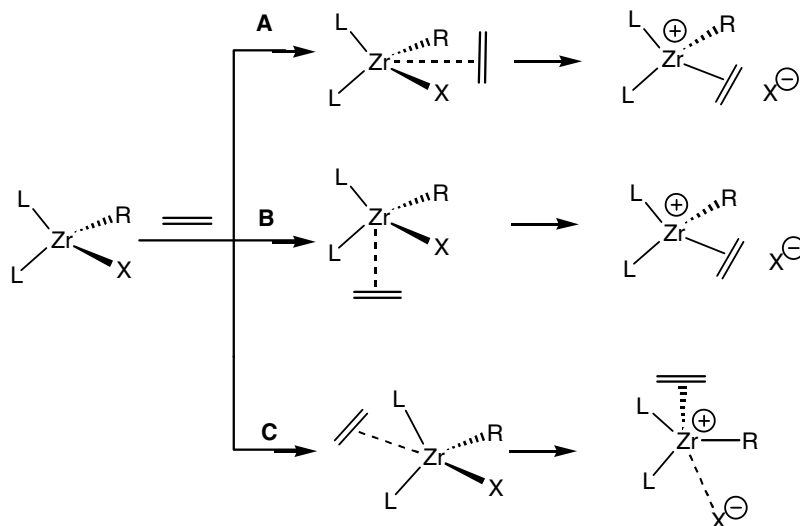


These investigations were carried out using zirconium-methyl complexes, although methyl ligands have a specific chemistry (cf. Scheme 3) and are rather poor models of the growing polymer chain. Bulkier alkyl ligands give much higher anion exchange rates, e.g., in the series (1,2-Me₂Cp)₂Zr(R)(μ-Me)B(C₆F₅)₃ (**12**) the reorganisation enthalpies decrease sharply with increasing bulkiness of the alkyl ligand, R = Me > CH₂Bu^t > CH₂-

SiMe₃ ≫ CH(SiMe₃)₂ [50]. For the *ansa*-zirconocenes **13**, rates for R = CH₂SiMe₃ are approximately four times higher than for R = Me, with values of ca. 20 s⁻¹ for X = MeB(C₆F₅)₃ and 800 s⁻¹ for X = B(C₆F₅)₄. The data also indicate that the “chain swinging” event associated with anion exchange involves a 180° rotation of the alkyl ligand [51].



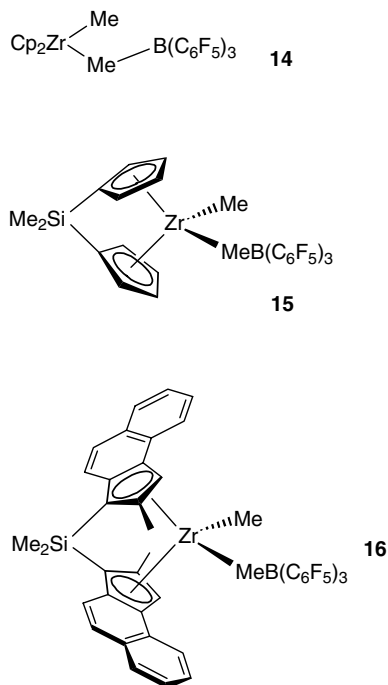
The monomer approach can occur from a head-on direction (Scheme 9, path A), from the same side as the anion (path B), or from a position *trans* to the anion, with side exchange of the alkyl ligand R (path C). DFT calculations on the ion pair [(1,2-Me₂Cp)₂ZrR⁺⋯B(C₆F₅)₄⁻] (R = Me, Et) have suggested that ethene-sandwiched π-complexes are formed via A and B, and a non-sandwiched π-complex via C. The product of path C, arising from C₂H₄ attack on the metal centre *trans* to the anion in an S_N2-type reaction, was found to be the most stable by 3.5 kcal/mol [52]. Calculations by Lanza and Fragalà [53] on a simplified model of the constrained-geometry catalyst, (C₅H₄SiH₂NMe)TiMe⁺MeB(C₆F₅)₃⁻, ruled out paths A and B and suggested the monomer approach via path C, i.e., from the side opposite to the anion, as the favoured insertion pathway. This reaction sequence minimises cation–anion separation and allows facile anion re-coordination once the insertion step is complete. By contrast, calculations



Scheme 9.

by Nifant'ev et al. [54] on $\text{Cp}_2\text{ZrEt(X)} + \text{C}_2\text{H}_4$ suggested path A as the preferred route for anion substitution by the olefin.

In an attempt to provide evidence of the stereochemical course, rates and equilibrium positions of anion displacement, Brintzinger and co-workers [55] studied the reactions of a series of zirconocene methylborates, including **14–16**, with weak donors, notably *N,N*-dimethylaniline (DMA) and di-*n*-butyl ether (DBE).



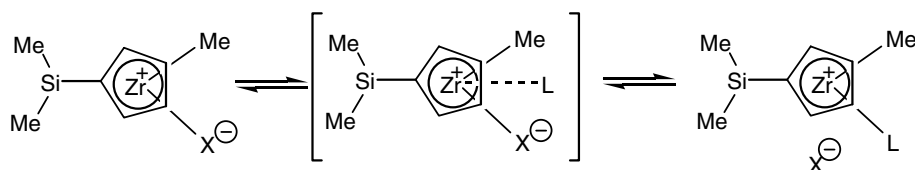
Anion substitution with these donors is reversible. Indenyl and benzindenyl complexes did not react with DMA. Whereas the equilibrium constants $K = [\text{ZrMe(L)}^+\text{X}^-]/[\text{ZrMe(X)}] \cdot [\text{L}]$ changed only by a factor of five from the most open (**15**) to the most bulky ligand system (**16**), the second-order displacement rate constants changed by five orders of magnitude, from $0.03 \text{ L mol}^{-1} \text{ s}^{-1}$ for **16** to $4000 \text{ L mol}^{-1} \text{ s}^{-1}$ for **15** (at 300 K). The rates of anion displacement proved particularly sensitive to substituents in 2-position on the cyclopentadienyl ring. The reaction shows several features that are likely to be important for the mechanism of polymerisation catalysis: (i) The reaction proceeds via an associa-

tive, $\text{S}_{\text{N}}2$ -type mechanism; (ii) anion substitution is stereospecific: the donor ligand L occupies the site the anion has left, without site-exchange of the methyl ligands; (iii) on addition of L, the anion is retained in an outer-sphere complex; solvated, separated ions are not formed in hydrocarbon solvents; (iv) exchange of outer-sphere and inner-sphere anions shows the same stereospecificity as anion displacement by the donor ligand; this process is much faster than methyl site exchange.

Semi-empirical and DFT calculations suggested a front-attack by L on the metal centre, which readily explains the observed retention of configuration during the substitution process (Scheme 10). The same structural type is also favoured for L = ethene or propene. Significantly, the experimental results on the stereochemistry of anion displacement as well as these calculations are in contrast to the theoretical models by Ziegler and Fragalá [52,53]. The relative positions of cation and anion in these ion pairs are quite similar to those found in the solid-state structures of $[\text{Cp}^{\text{R}}\text{HfMe}_2(\text{toluene})]^+ [\text{MeB}(\text{C}_6\text{F}_5)_3]^-$ ($\text{Cp}^{\text{R}} = 1,3\text{-C}_5\text{H}_3(\text{SiMe}_3)_2, \text{C}_5\text{Me}_5$) [39,40] and suggested very recently on the basis of NMR investigations for outer-sphere ion pairs in solution [49].

The rate of anion substitution k_{sub} strongly depends on the ligand framework and was found to be particularly slow for those complexes known to be the most effective catalysts for propene polymerisation, i.e., for **13** ($\text{R} = \text{Me}, \text{X} = \text{MeB}(\text{C}_6\text{F}_5)_3$) $k_{\text{sub}} = 8 \text{ L mol}^{-1} \text{ s}^{-1}$, while the value for **16** is even lower, $k_{\text{sub}} = 0.03 \text{ L mol}^{-1} \text{ s}^{-1}$. If these data are applicable to catalytic systems, the results would point towards a rather slow initiation. The reverse reaction, the rate of displacement of DBE by $\text{MeB}(\text{C}_6\text{F}_5)_3^-$, is even slower: 0.005 s^{-1} and $2.7 \cdot 10^{-5} \text{ s}^{-1}$ for **13** and **16**, respectively. Polymerisation rates with such catalysts are typically many orders of magnitude higher. Even if it can be expected that the anion can compete much more effectively with alkene ligands than with DBE, these slow rates of anion re-association have led the authors to suggest that this is an infrequent event that impedes further propagation. This would hold particularly for the even less nucleophilic $\text{B}(\text{C}_6\text{F}_5)_4^-$. Chain growth would therefore be initiated by anion displacement, followed by rapid monomer uptake and slow anion re-coordination.

This view of the chain growth process gains support by the observation that the molecular weight of polypropene samples produced with “constrained-geometry” titanium catalysts is 10 times higher if the counteranion

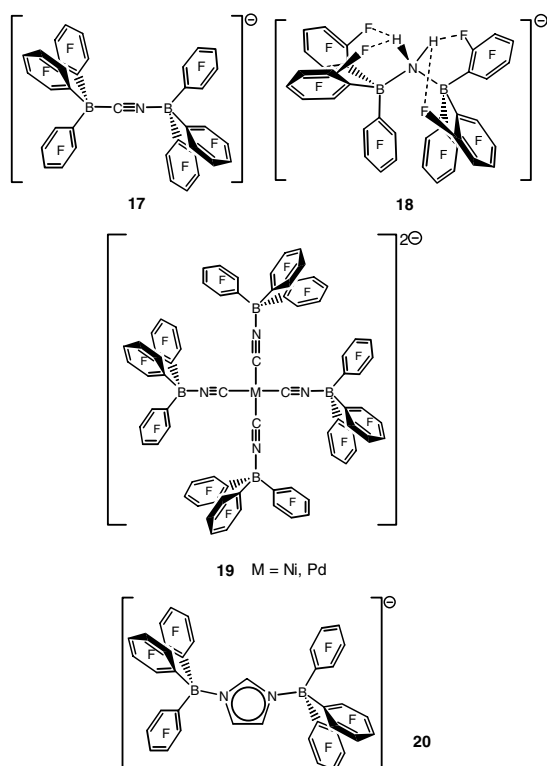


Scheme 10.

is $\text{B}(\text{C}_6\text{F}_5)_4^-$ than with the more strongly coordinating $\text{MeB}(\text{C}_6\text{F}_5)_3^-$ [34]. On the other hand, the idea of a “spectator” role for the anion during the polymerisation process and very slow anion re-association is not supported by kinetic studies (vide infra).

4. Controlling catalyst activity: Quantification of anion effects

In view of the importance of the counteranion on catalyst activity, a number of reports have been concerned with the assessment of anion effects [28,56]. Certainly different activator systems can have most remarkable effects on catalyst performance; for example, activating the catalyst precursor (SBI)ZrCl₂ with TIBA and $[\text{CPh}_3][\text{CN}\{\text{B}(\text{C}_6\text{F}_5)_3\}_2]$ instead of MAO led to a 30–40 fold increase in ethene polymerisation activity [57]. Some clear trends are apparent, such as the decrease in the strength of anion binding in the series $\text{MeB}(\text{C}_6\text{F}_5)_3^- > \text{MeB}(\text{C}_6\text{F}_4\text{-}2\text{-C}_6\text{F}_5)_3^- > \text{B}(\text{C}_6\text{F}_5)_4^-$ which is reflected in an increase in polymerisation activity within the same series. Examples of anions designed to maximise charge delocalisation and minimise coordinative tendencies are 17–20 [34,57,58]. However, in most cases a strict comparison between different catalyst systems is not possible since concentrations and reaction times were varied within wide limits. Differences in reaction conditions have, for example, led to activities being reported for the “standard” $\text{Cp}_2\text{ZrCl}_2/\text{MAO}$ catalyst that vary over four orders of magnitude [18].



Much effort has been directed towards the design of new metallocenes for ethene polymerization, and catalyst activities are often directly correlated with ligand structure [59]. However, the productivity of polymerization catalysts is a function of many variables, of which the nature of the ligand may not be the most important. Several scenarios are possible: (a) A catalyst may have an intrinsically high propagation rate k_p but the productivity is low because the activation method is inefficient and only generates very low concentrations of active species $[\text{C}^*]$; (b) the activation is efficient but the equilibrium between active and dormant species is unfavorable (e.g., because of tight cation–anion interaction, solvent coordination, etc.); (c) catalyst activation is efficient and $[\text{C}^*]$ is high but a facile decomposition pathway leads to early catalyst deactivation; (d) the catalyst may form high $[\text{C}^*]$ and give intrinsically high chain propagation rates, but the monomer concentration becomes depleted over the duration of the experiment, or the delivery of monomer to the active centre is too slow (i.e., mass-transport limitation); (e) as for (d), but the polymer is poorly soluble, begins to precipitate during the early stages of the reaction and thereby removes catalyst from the reaction; (f) activation is efficient, the polymerization is not mass-transport limited, and catalyst productivity is a function of the ligand employed.

It is clear that although most catalytic experiments tend to assume that situation (f) prevails, this is not necessarily achieved. Differences in catalyst activation and reaction conditions can produce differences in catalyst activities which are at least as important as changes in ligand structure. A major problem is mass-transport limitation under conditions typically employed for catalyst testing under laboratory conditions, i.e., with toluene solutions under 1 bar monomer pressure at 25–50 °C. Ethene in particular has very limited toluene solubility, and monomer uptake from the gas phase is remarkably slow. An additional problem in that case is the precipitation of the polymer at an early stage, which tends to co-precipitate some catalyst and prevents a quantitative assessment of activities. This is also important, though less problematic, for propene. For reliable activity data it needs to be demonstrated that diffusion limitation is absent, e.g., by plotting the dependence of polymer yield on the catalyst concentration [34,60].

Propene polymerisations using a given catalyst, (SBI)ZrMe₂, allowed the determination of the anion-dependence of catalyst activities under strictly comparable conditions. Since catalyst productivity values of metallocenes generally decrease with increasing zirconocene concentration, the data were extrapolated to $[\text{Zr}] = 0$ to arrive at the “intrinsic” activities, which should be independent of catalyst concentration (although still dependent on temperature and solvent) and provide a

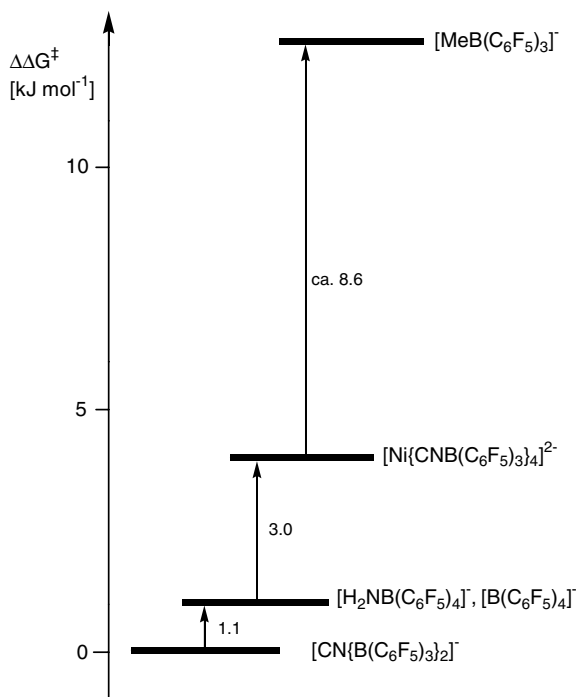


Fig. 1. Activation energy increments for a series of perfluoroarylborate anions in propene polymerisations with (SBI)ZrMe₂/TIBA/[CPh₃][X] (toluene, 25 °C, 1 bar).

characteristic determinant of the anion influence. Taking the least coordinating anion, [CN{B(C₆F₅)₃}₂]⁻ (**17**), as the baseline, these data provide an estimate of the activation energy increment that each anion provides (Fig. 1) [34]. The more strongly coordinating MeB(C₆F₅)₃⁻ anion gave catalysts that were too poorly active to operate on the same timescale employed for the trityl activators (reaction times of 10–30 min vs. 30 s); i.e., the activation barrier for MeB(C₆F₅)₃⁻ is ca. 12 kJ/mol higher than for [CN{B(C₆F₅)₃}₂]⁻.

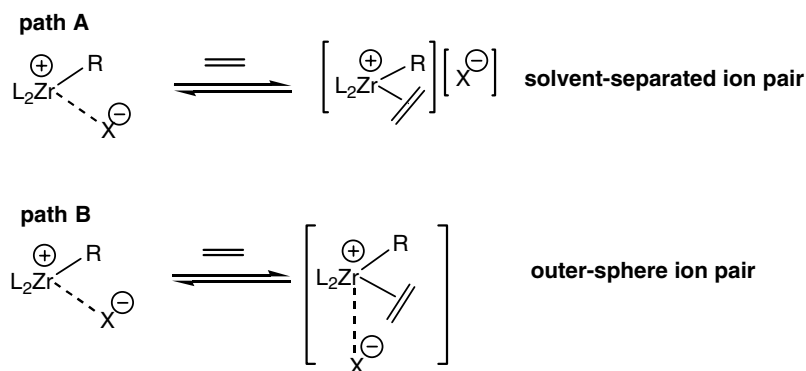
The amidodiborate anion [H₂N{B(C₆F₅)₃}₂]⁻ (**18**), although of similar size to [CN{B(C₆F₅)₃}₂]⁻, is comparable to B(C₆F₅)₄⁻ in catalytic activity, a possible

consequence of its bent and more polar structure [61]. While at 25 °C the cyano-bridged anion [CN{B(C₆F₅)₃}₂]⁻ was found to give the highest propene polymerisation activities, at 60 °C [H₂N{B(C₆F₅)₃}₂]⁻ proved superior, probably do to its greater thermal stability [62].

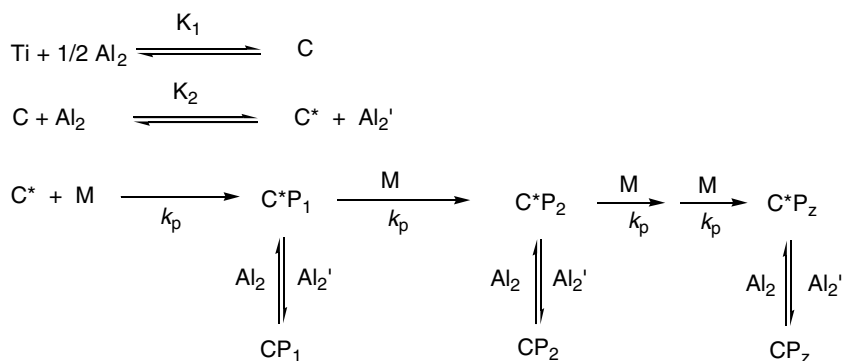
The observed anion effects on the catalytic activity can be interpreted in two ways: (1) the activity increases because the less coordinating anion generates higher concentrations of active species, or (2) the anion modulates the activation energy, i.e., remains involved in the transition state. The first case implies the “solvated ion pair” model for the active species (Scheme 11, path A), whereas in the latter there the anion remains associated in the outer coordination sphere (path B). Information about this aspect of the polymerisation mechanism is obtained by kinetic studies.

5. Polymerisation kinetics

Early studies by Fink et al. on the mechanism of ethene polymerisation using a combination of quenched-flow kinetic [63] and ¹³C NMR spectroscopic techniques [64,65] on the systems Cp₂TiRCl/AIR₂Cl/ethene (R = Me, Et) clearly showed (i) the formation of a chloro-bridged adduct between the aluminium and titanium component (“primary complex”), (ii) that initiation was significantly slower than propagation, i.e., that polymer chains were formed before most of the Ti–Me bonds had undergone the first insertion; (iii) that the primary complex was not itself the active species; (iv) that the active species was in equilibrium with an observable stabilised species, i.e., a resting state, and (v) that a titanium ethene π-complex (cf. Schemes 6 and 11), although mechanistically necessary, was not present in detectable quantities. These observations formed the basis of a general mechanism where polymer chain growth proceeded stepwise and could be interrupted at any stage by reversibly forming a resting state:



Scheme 11.



Scheme 12. C = catalyst precursor, C* = active catalyst species, P_z = polymer chain. C*P_z denotes active species carrying polymeryl chain after z monomer insertions, in equilibrium with the resting state CP_z. Adapted from [65].

the “intermittent growth” model (Scheme 12) [65]. A characteristic feature is expressed by the relative rate constants for the first few ethene insertions into titanium–alkyl bonds: insertion into Ti–Me was 120 times slower than insertion into Ti–Et and 96 times slower than into Ti–Prⁿ; in other words, the catalyst initiation step is concerned with the conversion of the Ti–Me precursor into the next higher alkyl before rapid chain growth ensues [64].

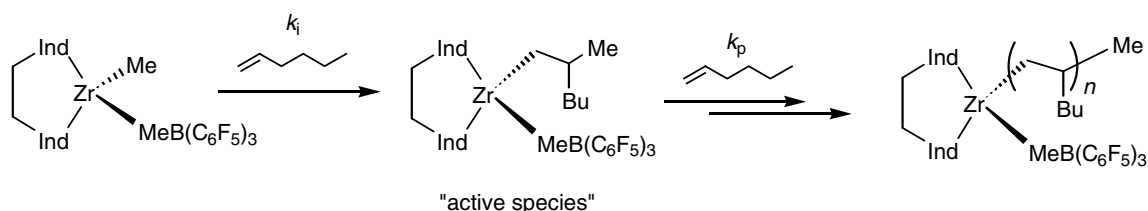
More recently, Landis and co-workers [66] studied the polymerisation of 1-hexene with (EBI)ZrMe(μ-Me)B(C₆F₅)₃ in toluene [EBI = *rac*-C₂H₄(Ind)₂]. In line with Fink’s results, they defined the catalyst initiation step as the (irreversible) first monomer insertion into the Zr–Me bond (Scheme 13). The first and subsequent insertion products were regarded as the “active species”, the concentration of which was determined by deuterium quenching and approached 100%. According to this definition, the active species is a higher metal alkyl where the anion still occupies the coordination site required for alkene binding. This definition differs from the one preferred by Song et al. [67] who attempted to differentiate between the total concentration of Zr species carrying a polymeryl chain and those actively engaged in polymer chain growth at any given time.

The hexene polymerisation follows a rate law that is first order in both catalyst and monomer. Chain propagation was ca. 30 faster than initiation, with $k_p \approx 6 \text{ L mol}^{-1} \text{ s}^{-1}$ (at 20 °C). Unlike the Fink model, no pooling

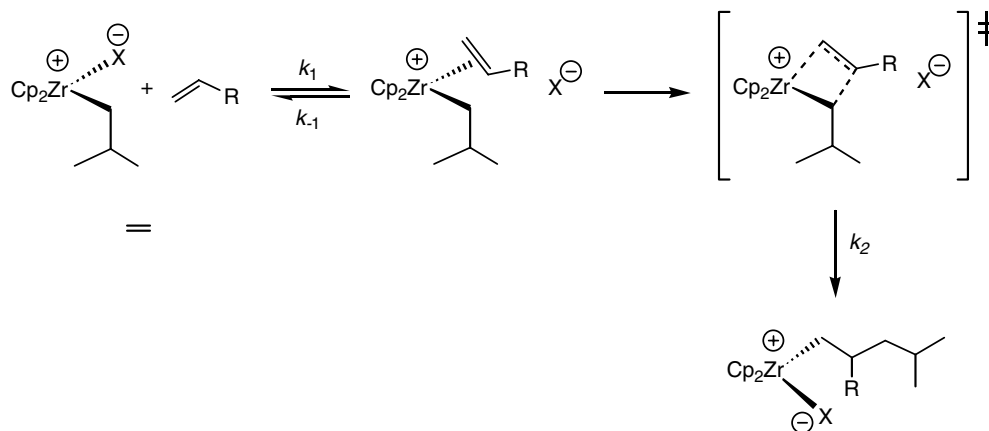
of the catalyst into a dormant state was evident; > 90% of [Zr]_{total} carried a polymeryl chain, with 1,2-insertions leading to >99% isotactic poly(hexene) [66].

Heavy-atom (¹²C/¹³C) kinetic isotope effects (KIE) for an (EBI)ZrMe₂/activator system were consistently higher for the hexene-C₂ carbon than for C₁ and negligible for C atoms 3–5. The results, in comparison with computed KIE’s, were in agreement with an equilibrium reaction for hexene binding, followed by an irreversible insertion step (Scheme 14). Since the same isotope effect was observed for different activators [B(C₆F₅)₃, Al(C₆F₅)₃, HNMe₂Ph⁺B(C₆F₅)₄[−], MAO], in spite of widely varying catalyst productivities, it was concluded that the transition states must have very similar structures in all cases [68]. Although this could be seen to question the influence of the counteranion on the transition state energy, the results suggest in essence that in all these cases the transition state involves the same reaction step, i.e., the transfer of an alkyl ligand to the C₂-atom of the monomer.

The reaction of (EBI)ZrMe(μ-Me)B(C₆F₅)₃ with 1-hexene at 40 °C results in partial conversion of the methyl complex into a Zr–poly(hexene) (Zr–PH) species [69]. The first insertion step was 400 times slower than subsequent insertions; propagation was 4×10^4 times faster than termination. The polymerisation is living under these conditions, and observation of the disappearance of Zr–¹³CH₂–POL on addition of a few equivalents of unlabelled 1-hexene was in agreement with a “continuous” insertion mechanism where each hexene



Scheme 13.



Scheme 14.

insertion step is followed by anion re-association, in contradiction to Brintzinger's suggestions [55] of slow anion re-coordination.

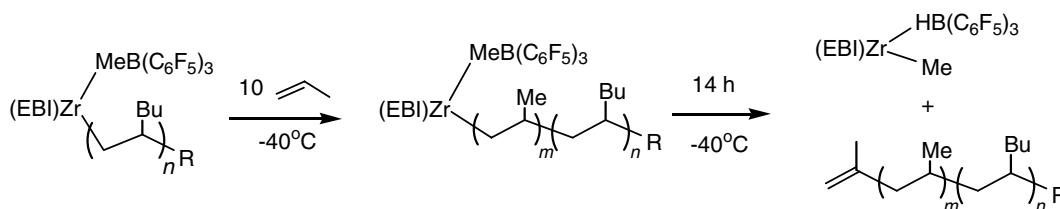
The addition of propene to the Zr-PH species led to the formation of a Zr-PP-*b*-PH block copolymer. Surprisingly at first glance, the rate of propene polymerisation was only three times faster than that of 1-hexene. This slow rate is caused by the strongly coordinating nature of $\text{MeB}(\text{C}_6\text{F}_5)_3^-$ and contributes to the high regioselectivity of the polymerisation: no 2,1-propene misinsertions were detected. Termination occurs by β -H elimination in a first-order process (Scheme 15). It could also be shown that chain end epimerisation proceeded via a zirconium *tert*-alkyl (rather than π -allyl) intermediate [70,71].

By contrast to hexene polymerisations with $(\text{EBI})\text{Zr-Me}(\mu\text{-Me})\text{B}(\text{C}_6\text{F}_5)_3$, the polymerisation of propene with the system $(\text{SBI})\text{ZrMe}_2/\text{TIBA}/[\text{CPh}_3][\text{CN}\{\text{B}(\text{C}_6\text{F}_5)_3\}_2]$ is orders of magnitude faster, too fast to be followed by variable-temperature NMR spectroscopy, and not living. Song et al. [67] studied the kinetics of this system by quenched-flow techniques in toluene at 25 ± 0.1 °C under 1 bar propene over reaction times of 0.2–5 s and estimated the rates of initiation, chain propagation and chain termination. Since the isotactic polypropylene (*i*-PP) produced has limited solubility in toluene, reaction times were limited by the onset of polymer precipitation. The polymerisation is first-order in $[\text{C}_3\text{H}_6]$ and $[\text{Zr}]$.

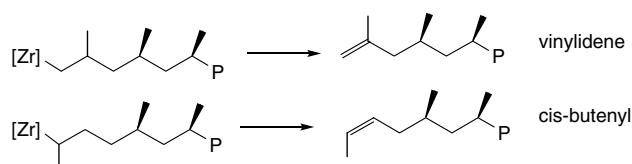
NMR studies confirmed that by using an excess of TIBA all the $(\text{SBI})\text{ZrMe}_2$ precursor complex was converted to other species, and the limitation imposed by the known slow first monomer insertion into the Zr-Me bond did not apply. Nevertheless, this early reaction phase does not operate under steady-state conditions. The catalyst initiation rate constant proved difficult to determine with accuracy; from the time-dependence of PP yield, $k_i \approx 5 \text{ L mol}^{-1} \text{ s}^{-1}$. Since the half-life $t_{1/2}^{\text{init}}$ for this initial phase was $0.24 \pm 0.03 \text{ s}$, after a reaction time of 1 s catalyst initiation was no longer kinetically relevant.

Two propagation rate constants were determined. The time dependence of polymer mass gives an “apparent” rate k_p^{app} , since the analysis assumes that 100% of the initial Zr precursor has become catalytically active; $k_p^{\text{app}} \approx (1.3\text{--}1.9 \pm 0.1) \times 10^3 \text{ L mol}^{-1} \text{ s}^{-1}$, with the lower values found for the higher catalyst concentration where monomer depletion effects are felt. For comparison with the hexene data discussed above, at $[\text{C}_3\text{H}_6] = 0.59 \text{ M}$ this corresponds to an observed first-order rate $k^{\text{obs}} = 760\text{--}1100 \text{ s}^{-1}$. Chain transfer to aluminium was negligible.

By contrast, the rate of polymer chain growth was an order of magnitude faster, and from determinations of the number-average molecular weight M_n a propagation rate of $k_p = (17.2 \pm 1.4) \times 10^3 \text{ L mol}^{-1} \text{ s}^{-1}$ was determined. Since the latter is independent of $[\text{Zr}]$, the ratio k_p/k_p^{app} gives a measure of the mol-fraction of total $[\text{Zr}]$ that is actively engaged in chain growth at any



Scheme 15.



one time, in this case $k_p/k_p^{\text{app}} = 0.08$. In other words, about 90% of total zirconocene was in some sort of dormant state. The termination rate was $k_t \approx 9 \text{ s}^{-1}$.

The nature of the dormant state was determined by end-group analysis. Two types of terminal unsaturations were found, even in polymers made over reaction times of less than 1 s: vinylidene end groups arising from 1,2-inserted polymeryl chains, and *cis*-butenyl end groups, arising from 2,1-misinsertions (Scheme 16). The latter were dominant (66%). Low levels of stereoerrors due to enchainment 2,1-misinsertions were also detected, about 1 in 500. The data suggested that 2,1-insertion is slow but leads to the accumulation of dormant states carrying Zr-*sec*-alkyl chains which either terminate or undergo slow 1,2-propene insertions to re-enter the main propagation sequence.

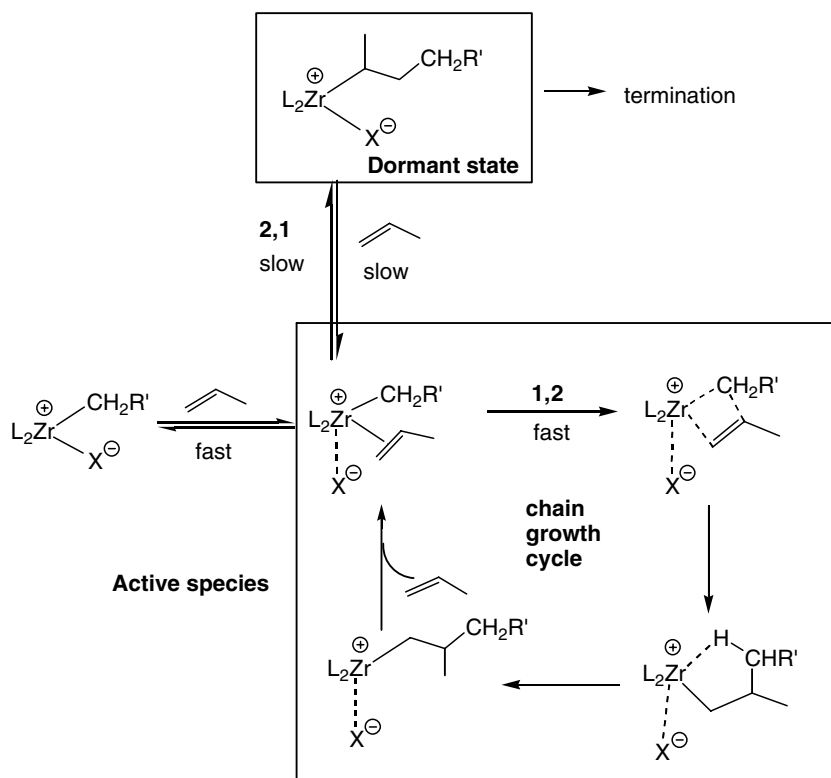
Very similar kinetics were observed for (SBI)ZrCl₂/MAO: although this catalyst is an order of magnitude less productive, the concentration of active species turned out to be almost identical to the borate system:

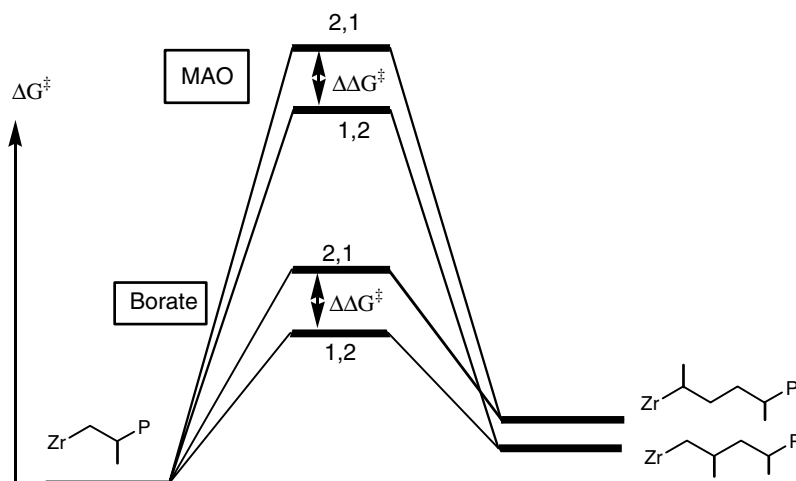
$k_p/k_p^{\text{app}} = 0.08$, with a similar accumulation of dormant states due to 2,1-misinsertions.

If the monomer binding equilibrium between [(SBI)Zr(R)⁺···X⁻] and [(SBI)Zr(R)(propene)⁺···X⁻] is established sufficiently fast, the results suggest an equilibrium between active and dormant states (Scheme 17).

Based on the results for this particular catalyst system at least, the energy difference between 1,2- and 2,1-propene insertion, $\Delta\Delta G^\ddagger$, is essentially independent of the nature of the anion (Scheme 18), whereas the anion influence on the chain propagation rate is significant.

The propene insertion rates determined for the (SBI)ZrMe₂/TIBA/trityl borate catalyst system at 25 °C ($k_p^{\text{obs}} \approx 10^4 \text{ s}^{-1}$) [67] are about an order of magnitude higher than the fastest anion exchange rates observed under comparable conditions. Unless there is a dramatic increase in anion mobility during the monomer insertion process, it seems likely therefore that the results point towards the existence of two kinetic regimes: (1) where monomer insertion is slower than anion exchange ($k_p \ll k_{\text{ips}}$), as in the case of 1-hexene polymerisation, and (2) where $k_p \gg k_{\text{ips}}$, as in fast ethene and propene polymerisations. In the latter case at present understanding, the fast chain growth is most conveniently explained by anion substitution followed by a series of monomer insertions (Fink–Brintzinger model), before anion re-association can take place and interrupt the process. Since these propene reactions are extremely





Scheme 18. Qualitative energy levels illustrating the formation of similar proportions of 1,2- and 2,1-insertions in trityl borate (lower set) and MAO-activated propene polymerisations (upper set).

fast, NMR monitoring of the Zr-polymeryl species and direct proof of the kinetic regime, as was possible for hexene polymerisations [69], has not been possible.

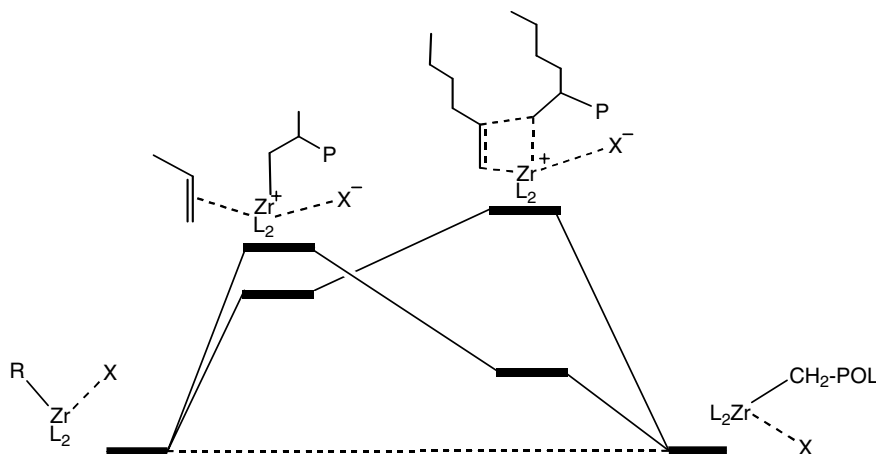
The existence of different kinetic regimes for closely related reactions is also demonstrated by a comparison of the anion effects in propene and 1-hexene polymerisations catalysed by (SBI)Zr(CH₂SiMe₃)(X) [X = MeB(C₆F₅)₃ and B(C₆F₅)₄]. These zirconium alkyls form very stable ion pairs which allow kinetic studies without TIBA scavenger. Propene polymerisations with X = B(C₆F₅)₄ were 70 times faster than for X = MeB(C₆F₅)₃, as expected for anions of different coordination power. However, hexene polymerisation rates differ only by a factor of three. This points towards an early transition state for propene, where anion substitution is important in the rate-limiting step, while for 1-hexene the transition state involves primarily the transfer of the (sterically more hindered) alkyl chain to the (also more

hindered) monomer and occurs later on the reaction coordinate (Scheme 19) [72].

On the other hand, 1-hexene polymerisations with (EBI)ZrMe(X) show a much stronger anion effect, with a 20-fold acceleration for X = B(C₆F₅)₄ over X = MeB(C₆F₅)₃ [73]. Such differences underline the remarkably subtle responses of metallocene catalysts to slight changes in ligand structure.

6. Anions and polymer stereochemistry

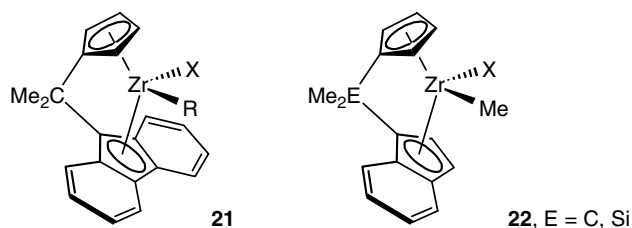
The anions discussed above are of considerable size and can therefore be expected to exert a significant influence on the stereochemistry of alkene polymerisation, even though the formation of syndiotactic and isotactic 1-alkenes have been readily explained by considering only the cationic metallocenium species and their ligand structure [74–76]. An example are the complexes



Scheme 19.

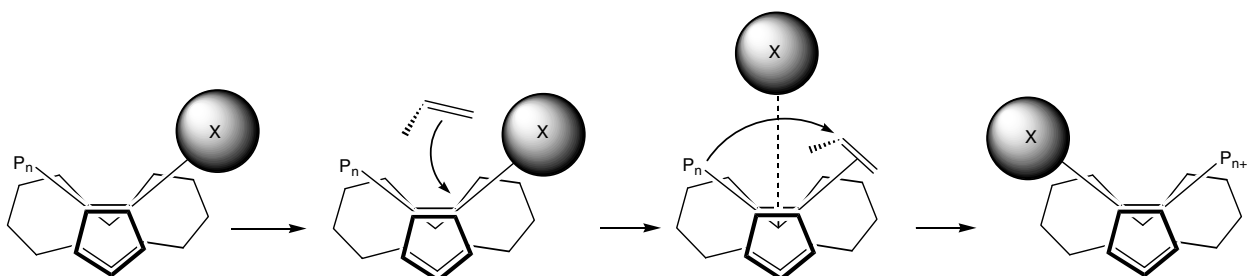
$\text{Me}_2\text{C}(\text{C}_5\text{H}_3\text{R})(\text{Fluorenyl})\text{ZrCl}_2$, the selectivity of which [syndiotactic ($\text{R} = \text{H}$); hemiisotactic ($\text{R} = \text{Me}$); isotactic ($\text{R} = \text{Bu}'$)] is conveniently explained using the “gas phase cation” model [77,78].

There is no detectable effect of the counteranion on polypropenes produced with C_2 -symmetric *ansa*-zirconocenes [62,79]. For the C_s -symmetric complex **21**, on the other hand, there is a pronounced increase in stereoselectivity with tighter ion pairing. In early work Herfert and Fink [80] showed that the activity of MAO-activated **21** ($\text{R} = \text{X} = \text{Cl}$) increases linearly with the dichloromethane content of the solvent, i.e., with the dielectric constant, while at the same time the intensities of the *rrrr* pentads decreased sharply and the *rmrr* pentads increased. This was interpreted in terms of formation of solvated ion pairs at high $[\text{CH}_2\text{Cl}_2]$ which allow more facile site epimerisation (“chain swinging”, cf. Scheme 7) than tight ion pairs. Similar observations were made more recently by Deffieux and co-workers [81] for the 1-hexene polymerisation with **21**/MAO, by Chen and Marks using the catalysts **21** [$\text{R} = \text{Me}$; $\text{X} = \text{MeB}(\text{C}_6\text{F}_5)_3$, $\text{MeB}(\text{C}_{12}\text{F}_9)_3$, $\text{MeB}(\text{C}_6\text{F}_5)_3$ and $\text{FAl}(\text{C}_{12}\text{F}_9)_3$] [82] and by Busico et al. [83] using the system **21**- Cl_2 /TIBA/[HNMe_2Ph][$\text{B}(\text{C}_6\text{F}_5)_4$]: high syndio-selectivity in toluene, particularly with $\text{FAl}(\text{C}_{12}\text{F}_9)_3^-$, and fast site epimerisation with collapse of *rrrr* intensity in polar solvents. Busico estimated an insertion activation energy in toluene of 10–15 kcal/mol and an activation energy for site epimerisation of about 20–25 kcal/mol, with both values reduced by 5–10 kcal/mol in bromobenzene. The *rrrr* pentad intensities for different anions are determined by the ratio of the rate of insertion to the rate of inversion. Remarkably, there is essentially no anion effect with catalyst **22** where inversion (chain swinging) is always much faster than propagation [84].



It is clear therefore that close proximity of the anion is required to suppress chain swinging and to ensure stereoregular chain propagation. Equally, syndiospecific propagation (Scheme 20) can only be explained if alkene attack from the side opposite the anion does not occur, even though earlier calculations favoured exactly this route because it minimises cation–anion separation [52,53]. It seems therefore that the highly stereoselective sequence: anion substitution–insertion/chain migration – anion association to the opposite site – requires a remarkable degree of molecular acrobatics.

Anion effects were also found important in the non-bridged zirconocenes $\text{ZrCl}_2(2\text{-ArInd})$ ($\text{Ar} = \text{aryl}$) which are thought to oscillate between *rac*- and *meso*-like states and are capable of producing elastomeric PP homopolymers [85,86]. It was suggested that these materials contain isotactic blocks which are responsible for the observed physical properties. Both the productivities and stereoselectivities (*mmmm* pentads) were found to be highest with MAO as catalyst activator and decrease in the sequence $\text{MAO} > [\text{HNMe}_2\text{Ph}][\text{B}(\text{C}_6\text{F}_5)_4]^- > \text{B}(\text{C}_6\text{F}_5)_3$. They are however rather sensitive to other factors, such as the type and previous history of the MAO employed [86]. Although there is evidence that the 2-phenylindenyl complex does indeed form polymers with stereoblocks [87], the polymer can be fractionated into an amorphous and essentially atactic major fraction and a minor, predominantly isotactic component [62,88,89]. The relative amount of the isotactic fraction is anion-dependent, $\text{MAO} < [\text{CN}\{\text{B}(\text{C}_6\text{F}_5)_3\}_2]^- \approx [\text{Ni}\{\text{CNB}(\text{C}_6\text{F}_5)_3\}_4]^{2-} < \text{B}(\text{C}_6\text{F}_5)_4^-$ and most probably produced by *rac*-like conformations. It has been suggested [88] that tighter anion binding in more ionic ion pairs increases the lifetime of the *rac*-like conformation and gives rise to the isotactic (*mmmm* ≈ 70 –80%) fraction. The size of the MAO-anion may be particularly relevant for these conformationally flexible catalysts; for example, Babushkin and Brintzinger [90] were able to show that zirconocenes exist as a mixture of tight ion pairs [$\text{Cp}_2\text{Zr}(\mu\text{-Me})_2\text{AlMe}_2^+ \cdots \text{MeMAO}^-$ and $\text{Cp}_2\text{ZrMe}^+ \cdots \text{MeMAO}^-$] in which the MeMAO^- anion has an effective hydrodynamic radius of 12.2–12.5 Å and may contain 150–200 Al atoms.



Scheme 20.

7. Conclusion

As this brief survey shows, metallocene catalysts based on well-defined ion pairs continue to make major contributions to our understanding of alkene polymerisation catalysis. The interplay of ligand structure and monomer- and anion-binding capacity is rather subtle and warns against facile generalisation of mechanistic aspects: what is important for one type of catalysts, such as solvent coordination or anion displacement, may not necessarily be extrapolated to other systems. The cooperation of different factors in order to slice small portions off the activation barrier is rather reminiscent of enzyme catalysis where precise tailoring of the active pocket and control of polar interactions are crucial. The ability to illustrate such factors in a precise manner is one of the major benefits of mechanistic studies in metallocene catalysis.

Acknowledgement

This work was supported by the European Commission (contract no. HPRN-CT2000-00004).

References

- [1] G. Wilkinson, P.L. Pauson, J.M. Birmingham, F.A. Cotton, *J. Am. Chem. Soc.* 75 (1953) 1011; G. Wilkinson, J.M. Birmingham, *J. Am. Chem. Soc.* 76 (1954) 4281.
- [2] K. Ziegler, H. Breil, E. Holzkamp, H. Martin, German Pat Appl. DBP973626 (18.11.1953); K. Ziegler, E. Holzkamp, H. Breil, H. Martin, *Angew. Chem.* 67 (1955) 426; K. Ziegler, E. Holzkamp, H. Breil, H. Martin, *Angew. Chem.* 67 (1955) 541; K. Ziegler, *Angew. Chem.* 76 (1964) 545.
- [3] G. Natta, P. Pino, E. Mantica, F. Danusso, G. Mazzanti, M. Peraldo, *La Chimica e l'Industria* 38 (1956) 124; G. Natta, *Angew. Chem.* 68 (1956) 393; G. Natta, *Angew. Chem.* 76 (1964) 553.
- [4] D.S. Breslow, US Pat. Appl. 537039 (1955); D.S. Breslow, N.R. Newburg, *J. Am. Chem. Soc.* 79 (1957) 5072.
- [5] G. Natta, P. Pino, G. Mazzanti, U. Giannini, *J. Am. Chem. Soc.* 79 (1957) 2975; G. Natta, P. Pino, G. Mazzanti, U. Giannini, E. Mantica, M. Peraldo, *J. Polym. Sci.* 26 (1957) 120.
- [6] W.P. Long, D.S. Breslow, *J. Am. Chem. Soc.* 82 (1960) 1953.
- [7] D.S. Breslow, N.R. Newburg, *J. Am. Chem. Soc.* 81 (1959) 81.
- [8] W.P. Long, *J. Am. Chem. Soc.* 81 (1959) 5312.
- [9] J.C.W. Chien, *J. Am. Chem. Soc.* 81 (1959) 86.
- [10] G. Henrici-Olivé, S. Olivé, *Angew. Chem. Int. Ed. Engl.* 6 (1967) 790.
- [11] A.K. Zefirova, A.E. Shilov, *Dokl. Akad. Nauk. SSSR* 136 (1961) 599; F.S. Dyachkovskii, A.K. Shilova, A.E. Shilov, *J. Polym. Sci. Part C* 16 (1967) 2333.
- [12] J.J. Eisch, A.M. Piotrovski, S.K. Brownstein, E.J. Gabe, F.L. Lee, *J. Am. Chem. Soc.* 107 (1985) 7219 (alkyne insertion into Ti-Me).
- [13] M. Bochmann, L.M. Wilson, *J. Chem. Soc., Chem. Commun.* (1986) 1610; M. Bochmann, L.M. Wilson, M.B. Hursthouse, R.L. Short, *Organometallics* 6 (1987) 2556; M. Bochmann, A.J. Jaggar, L.M. Wilson, M.B. Hursthouse, M. Motevalli, *Polyhedron* 8 (1989) 1838.
- [14] R.F. Jordan, C.S. Bajgur, R. Willet, B. Scout, *J. Am. Chem. Soc.* 108 (1986) 7410.
- [15] Review: R.F. Jordan, *Adv. Organomet. Chem.* 32 (1991) 325.
- [16] H. Sinn, W. Kaminsky, *Adv. Organomet. Chem.* 18 (1980) 99.
- [17] H. Schutenhaus, H.H. Brintzinger, *Angew. Chem. Int. Ed. Engl.* 18 (1979) 777; F.R.W.P. Wild, L. Zsolnai, G. Huttner, H.H. Brintzinger, *J. Organomet. Chem.* 23 (1982) 233.
- [18] P.C. Möhring, N.J. Conville, *J. Organomet. Chem.* 479 (1994) 1 (Cp cone angle and influence on polymerisations).
- [19] H.H. Brintzinger, D. Fischer, R. Mülhaupt, B. Rieger, R.M. Waymouth, *Angew. Chem. Int. Ed. Engl.* 34 (1995) 1143 (active species and stereoselectivity).
- [20] R.H. Grubbs, G.W. Coates, *Acc. Chem. Res.* 29 (1996) 85 (agostic interactions in olefin insertions).
- [21] M. Bochmann, *J. Chem. Soc., Dalton Trans.* (1996) 255 (cationic metallocene complexes).
- [22] W. Kaminsky, A. Laban, *Appl. Catal.* 222 (2001) 47; W. Kaminsky, *J. Chem. Soc., Dalton Trans.* (1998) 1413; W. Kaminsky, M. Arndt, *Adv. Polym. Sci.* 127 (1997) 144 (polymer materials via metallocenes).
- [23] A.L. McKnight, R.M. Waymouth, *Chem. Rev.* 98 (1998) (constrained-geometry catalysts).
- [24] W. Kaminsky (Ed.), *Metalorganic Catalysts for Synthesis and Polymerization: Recent Results by Ziegler-Natta and Metallocene Investigations*, Springer, Berlin, 1999.
- [25] T.J. Marks, J.C. Stevens (Eds.), *Topics Catal.* 7 (1999) 1–208 (special issue on metallocene and related catalysts).
- [26] J. A. Gladysz (Ed.), *Chem. Rev.* 100 (2000) 1167–1604 (special issue on soluble polymerisation catalysts).
- [27] M. Bochmann, A.J. Jaggar, J.C. Nicholls, *Angew. Chem. Int. Ed. Engl.* 29 (1990) 780; M. Bochmann, A.J. Jaggar, *J. Organomet. Chem.* 424 (1992) C5.
- [28] E.Y.X. Chen, T.J. Marks, *Chem. Rev.* 100 (2000) 1391.
- [29] A.G. Massey, A.J. Park, F.G.A. Stone, *Proc. Chem. Soc. [London]* (1963) 212; A.G. Massey, A.J. Park, *J. Organomet. Chem.* 2 (1964) 245; J.L.W. Pohlmann, F.E. Brinckmann, *Z. Naturforsch. Teil B* 20b (1965) 5.
- [30] H.W. Turner, *Eur. Pat. Appl.* 277004 (1988, to Exxon).
- [31] X. Yang, C.L. Stern, T.J. Marks, *J. Am. Chem. Soc.* 113 (1991) 3623; J.A. Ewen, M.J. Elder, *Eur. Pat. Appl.* 427696 (1991).
- [32] M. Bochmann, S.J. Lancaster, *Angew. Chem. Int. Ed. Engl.* 33 (1994) 1634; M. Bochmann, S.J. Lancaster, *J. Organomet. Chem.* 434 (1992) C1.
- [33] S. Beck, M.H. Prosenc, H.H. Brintzinger, R. Goretzki, N. Herfert, G. Fink, *J. Mol. Catal. A: Chem.* 111 (1996) 67; T. Haselwander, S. Beck, H.H. Brintzinger, in: G. Fink, R. Mülhaupt, H.H. Brintzinger (Eds.), *Ziegler Catalysts*, Springer, Berlin, 1995, p. 181.
- [34] J. Zhou, S.J. Lancaster, D.A. Walker, S. Beck, M. Thornton-Pett, M. Bochmann, *J. Am. Chem. Soc.* 123 (2001) 223.
- [35] I. Tritto, R. Donetti, M.C. Sacchi, P. Locatelli, G. Zannoni, *Macromolecules* 30 (1997) 1247; I. Tritto, R. Donetti, M.C. Sacchi, P. Locatelli, G. Zannoni, *Macromolecules* 32 (1999) 264.

- [36] D.E. Babushkin, N.V. Semikolenova, V.A. Zakharov, E.P. Talsi, *Macromol. Chem. Phys.* 201 (2000) 558;
K.P. Bryliakov, N.V. Semikolenova, D.V. Yudaev, V.A. Zakharov, H.H. Brintzinger, M. Ystenes, E. Rytter, E.P. Talsi, *J. Organomet. Chem.* 683 (2003) 92;
K.P. Bryliakov, N.V. Semikolenova, V.A. Zakharov, E.P. Talsi, *J. Organomet. Chem.* 683 (2003) 23;
K.P. Bryliakov, N.V. Semikolenova, D.V. Yudaev, M. Ystenes, E. Rytter, V.A. Zakharov, E.P. Talsi, *Macromol. Chem. Phys.* 204 (2003) 1110;
K.P. Bryliakov, E.P. Talsi, M. Bochmann, *Organometallics* 23 (2004) 149.
- [37] M. Bochmann, S.J. Lancaster, *J. Organomet. Chem.* 497 (1995) 55.
- [38] Review: G. Erker, *Acc. Chem. Res.* 34 (2001) 309;
M. Dahlmann, G. Erker, K. Bergander, *J. Am. Chem. Soc.* 122 (2000) 7986;
J. Karl, M. Dahlmann, G. Erker, K. Bergander, *J. Am. Chem. Soc.* 120 (1998) 5643.
- [39] M. Bochmann, O.B. Robinson, S.J. Lancaster, M.B. Hursthouse, S.J. Coles, *Organometallics* 14 (1995) 2456.
- [40] D.J. Gillis, R. Quyoum, M.J. Tudoret, Q. Wang, D. Jeremic, A.W. Roszak, M.C. Baird, *Organometallics* 15 (1996) 3600;
D.J. Gillis, M.J. Tudoret, M.C. Baird, *J. Am. Chem. Soc.* 115 (1993) 2543.
- [41] J. Saßmannshausen, M. Bochmann, J. Rösch, D. Lilge, *J. Organomet. Chem.* 548 (1997) 23.
- [42] M.C. Baird, *Can. J. Chem.* 81 (2003) 330;
S.W. Ewart, M.C. Baird, *Topics Catal.* 7 (1999) 1.
- [43] L. Jia, X. Yang, C.L. Stern, T.J. Marks, *Organometallics* 16 (1997) 842.
- [44] P.A. Deck, T.J. Marks, *J. Am. Chem. Soc.* 117 (1995) 6128;
A.R. Siedle, R.A. Newmark, *J. Organomet. Chem.* 497 (1995) 119;
A.R. Siedle, B. Hanggi, R.A. Newmark, K.R. Mann, T. Wilson, *Macromol. Symp.* 89 (1995) 299;
P.A. Deck, C.L. Beswick, T.J. Marks, *J. Am. Chem. Soc.* 120 (1998) 1772.
- [45] S. Beck, S. Lieber, F. Schaper, A. Geyer, H.H. Brintzinger, *J. Am. Chem. Soc.* 123 (2001) 1483.
- [46] In the specific case of $\text{MeB}(\text{C}_6\text{F}_5)_3^-$, a second exchange pathway is possible via $\text{B}(\text{C}_6\text{F}_5)_3$ dissociation and recombination which leads to the permutation of Zr–Me and B–Me signals at the same rate as Cp and bridge signals. This is important in some cases but is excluded from the present discussion on ion mobility..
- [47] S. Beck, A. Geyer, H.H. Brintzinger, *Chem. Commun.* (1999) 2477.
- [48] N.G. Stahl, C. Zuccaccia, T.R. Jensen, T.J. Marks, *J. Am. Chem. Soc.* 125 (2003) 5256.
- [49] C. Zuccaccia, N.G. Stahl, A. Macchioni, M.C. Chen, J.A. Roberts, T.J. Marks, *J. Am. Chem. Soc.* 126 (2004) 1448.
- [50] C.L. Beswick, T.J. Marks, *J. Am. Chem. Soc.* 122 (2000) 10358.
- [51] F. Song, S.J. Lancaster, A. Macchioni, M. Bochmann, in preparation.
- [52] K. Vanka, T. Ziegler, *Organometallics* 20 (2001) 905;
Note added in proof: More recent calculations favour the head-on approach of monomers: Z.T. Xu, K. Vanka, T. Zeiger, *Organometallics* 23 (2004) 104.
- [53] G. Lanza, I. Fragalà, *Topics Catal.* 7 (1999) 45;
G. Lanza, I.L. Fragalà, T.J. Marks, *J. Am. Chem. Soc.* 122 (2000) 12764.
- [54] I.E. Nifant'ev, L.Y. Ustynyuk, D.N. Laikov, *Organometallics* 20 (2001) 5375.
- [55] F. Schaper, A. Geyer, H.H. Brintzinger, *Organometallics* 21 (2002) 473.
- [56] X. Yang, C.L. Stern, T.J. Marks, *J. Am. Chem. Soc.* 113 (1991) 3623;
Y.X. Chen, C.L. Stern, S. Yang, T.J. Marks, *J. Am. Chem. Soc.* 118 (1996) 12451;
Y.X. Chen, C.L. Stern, T.J. Marks, *J. Am. Chem. Soc.* 119 (1997) 2582;
L. Jia, X. Yang, C.L. Stern, T.J. Marks, *Organometallics* 16 (1997) 842.
- [57] S.J. Lancaster, D.A. Walker, M. Thornton-Pett, M. Bochmann, *Chem. Commun.* (1999) 1533.
- [58] R.E. LaPointe, G.R. Roof, K.A. Abboud, J. Klosin, *J. Am. Chem. Soc.* 122 (2000) 9560;
R.E. laPointe, *PCT Int. Appl. WO9942467* (1999).
- [59] See for example H.G. Alt, *J. Chem. Soc., Dalton Trans.* (1999) 1703;
H.G. Alt, A. Köppl, *Chem. Rev.* 100 (2000) 1205.
- [60] J. Saßmannshausen, M. Bochmann, J. Rösch, D. Lilge, *J. Organomet. Chem.* 548 (1997) 23.
- [61] S.J. Lancaster, A. Rodriguez, A. Lara-Sanchez, M.D. Hannant, D.A. Walker, D.L. Hughes, M. Bochmann, *Organometallics* 21 (2002) 451.
- [62] A. Rodriguez-Delgado, M.D. Hannant, S.J. Lancaster, M. Bochmann, *Macromol. Chem. Phys.* 205 (2004) 334.
- [63] G. Fink, D. Schnell, *Angew. Makromol. Chem.* 39 (1974) 131;
G. Fink, R. Rottler, D. Schnell, W. Zeller, *J. Appl. Polym. Sci.* 20 (1976) 2779;
G. Fink, W. Zoller, *Makromol. Chem.* 182 (1981) 3265;
G. Fink, D. Schnell, *Angew. Makromol. Chem.* 105 (1982) 31.
- [64] G. Fink, R. Rottler, R. Mynott, G. Fink, W. Fenzl, *Angew. Makromol. Chem.* 154 (1987) 1.
- [65] G. Fink, W. Fenzl, R. Mynott, *Z. Naturforsch. Teil B* 40b (1985) 158.
- [66] Z. Liu, E. Somsook, C.B. White, K.A. Rosaaen, C.R. Landis, *J. Am. Chem. Soc.* 123 (2001) 11193.
- [67] F. Song, R.D. Cannon, M. Bochmann, *J. Am. Chem. Soc.* 125 (2003) 7641.
- [68] C.R. Landis, K.A. Rosaaen, J. Uddin, *J. Am. Chem. Soc.* 124 (2002) 12062.
- [69] C.R. Landis, K.A. Rosaaen, D.R. Sillars, *J. Am. Chem. Soc.* 125 (2003) 1710.
- [70] D.R. Sillars, C.R. Landis, *J. Am. Chem. Soc.* 125 (2003) 9894.
- [71] J.C. Yoder, J.E. Bercaw, *J. Am. Chem. Soc.* 124 (2002) 2548.
- [72] F. Song, R.D. Cannon, M. Bochmann, *Chem. Commun.* (2004) 542.
- [73] C.R. Landis, Z. Lui, C.B. White, *Polym. Prepr.* 43 (2002) 301.
- [74] G.W. Coates, *Chem. Rev.* 100 (2000) 1223 (control of polyolefin stereoselectivity).
- [75] L. Resconi, L. Cavallo, A. Fait, F. Piemontesi, *Chem. Rev.* 100 (2000) 1253 (selectivity in propene polymerisation).
- [76] A.K. Rappé, W.M. Skiff, C.J. Casewit, *Chem. Rev.* 100 (2000) 1435 (modelling metallocene catalysts).
- [77] Y. van der Leek, K. Angermund, M. Reffke, R. Kleinschmidt, R. Goretzki, G. Fink, *Chem. Eur. J.* 3 (1997) 585.
- [78] K. Angermund, G. Fink, V.R. Jensen, R. Kleinschmidt, *Chem. Rev.* 100 (2000) 1457 (predicting stereospecificity of metallocene catalysts).
- [79] S. Hahn, G. Fink, *Macromol. Rapid Commun.* 18 (1997) 117.
- [80] N. Herfert, G. Fink, *Macromol. Chem.* 193 (1992) 773.
- [81] D. Coevoet, H. Cramail, A. Deffieux, *Macromol. Chem. Phys.* 200 (1999) 1208.
- [82] M.C. Chen, T.J. Marks, *J. Am. Chem. Soc.* 123 (2001) 11803.
- [83] V. Busico, R. Cipullo, F. Cutillo, M. Vacatello, V. van Axel Castelli, *Macromolecules* 36 (2003) 4258.
- [84] M. Mohammed, M. Nele, A. Al-Humydi, S. Xin, R.A. Stapleton, S. Collins, *J. Am. Chem. Soc.* 125 (2003) 7930.
- [85] G.W. Coates, R.M. Waymouth, *Science* 267 (1995) 217.

- [86] G.M. Wilmes, J.L. Polse, R.M. Waymouth, *Macromolecules* 35 (2002) 6766 and cited references.
- [87] V. Busico, R. Cipullo, A.L. Segre, G. Talarico, M. Vacatello, V. van Axel Castelli, *Macromolecules* 34 (2001) 8412.
- [88] V. Busico, R. Cipullo, W.P. Kretschmer, G. Talarico, M. Vacatello, V. van Axel Castelli, *Angew. Chem. Int. Ed.* 41 (2002) 505;
- V. Busico, V. van Axel Castelli, P. Aprea, R. Cipullo, A. Segre, G. Talarico, M. Vacatello, *J. Am. Chem. Soc.* 125 (2003) 5451.
- [89] W. Wiyatno, Z.R. Chen, Y. Liu, R.M. Waymouth, V. Krukoni, K. Brennan, *Macromolecules* 37 (2004) 701.
- [90] D.E. Babushkin, H.H. Brintzinger, *J. Am. Chem. Soc.* 124 (2002) 12869.